Nuclear Instruments and Methods in Physics Research A 764 (2014) 48–52

Contents lists available at ScienceDirect

Nuclear Instruments and Methods in Physics Research A

journal homepage: www.elsevier.com/locate/nima

Generation of energy bands in the electron beam with an asymmetric chicane-type emittance exchange beamline

Bo-Cheng Jiang*, Zhen-tang Zhao, Chao Feng

Shanghai Institute of Applied Physics, Chinese Academy of Sciences, Shanghai 201204, China

ARTICLE INFO

Article history:
Received 18 April 2014
Received in revised form
17 June 2014
Accepted 27 June 2014
Available online 10 July 2014

Keywords:
Emittance exchange
Energy bands
EEX-HHG
FEL

ABSTRACT

An asymmetric chicane-type transverse to longitudinal emittance exchange beam line is investigated and presented in this paper. This design is more feasible for existing machines due to its coaxial arrangement of the components and dispense of symmetric requirement of two doglegs compared to two-dogleg type one. By inserting quadrupoles between the dogleg and deflecting cavity, the dispersion can be amplified and hence the bending angle of the chicane is reduced with the same deflecting cavity parameters which will reduce the coherent synchrotron radiation effect.

1. Introduction

Transverse to longitudinal emittance exchange (EEX) has been proposed and widely investigated theoretically [1–4] and experimentally [5,6]. The EEX scheme is now beyond its original application of exchanging emittances between the transverse and the longitudinal planes to get smaller transverse emittance for free electron laser (FEL) purpose. The 4-D beam phase space manipulation is possible nowadays to meet the demands of various applications [7–10]. One of them is the generating high harmonic of the seed laser for producing short wave length FEL(EEX-HHG) [8,9]. In this scheme, an EEX beam line with a multi-slit mask at the entrance segments the beam into a series of beamlets separated in horizontal plane, which will produce energy bands at the exit of the beam line. After energy bands were created, the beam energy was modulated by a seed laser in a short undulator. The following chicane will convert energy modulation to longitudinal density modulation which will contain high harmonics of the seed laser. The scheme is similar to the echo-enabled harmonic generation scheme [11] for which the energy bands is created by an over suppressing chicane of an energy modulated bunch. The key technique of EEX-HHG is the energy bands generation using EEX beam line. This paper is following EEX-HHG scheme to investigate EEX capability of a new type beam line named as asymmetric chicane-type EEX beam line.

The EEX beam line proposed in [1] and experimentally demonstrated in [6] is a two-dogleg type EEX. In this case the beam line preceding and following the deflecting cavity is non-coaxial which places some obstacles for its adoption to the existing linac. Recently a chicane-type EEX beam line has been proposed [12] that an exact emittance exchange and even phase space exchange can be achieved by adding two quadrupoles before the deflecting cavity to change the sign of the dispersion function, thus one of the doglegs' bending angle can be reversed which makes the whole beam line coaxially. A forward step has been made to amplify the dispersion function which allows a reduction of RF deflecting voltage or a reduction of bending angles of the chicane magnets so as to match the EEX requirement $\eta^* k = -1 (\eta^* = -N\eta$, where η is the dispersion function of a half chicane, η^* is the amplified dispersion function see by the cavity, N is the amplification factor, k is the deflecting cavity strength parameter). This type of beam line is called a telescope EEX beam line.

In this paper, a novel idea is proposed, i.e. the doglegs preceding and following the deflecting cavity can be asymmetric. As long as $\eta^* k = -1$ is satisfied, an exact emittance exchange will be achieved for thin lens approximation. For such an asymmetric chicane-type emittance exchange beamline, the design will be more flexible. In this paper, we will show that only the first dogleg needs to match with input beam parameters. The second one can be flexible. The bending magnet can be weaker as long as there is enough drift space. The transfer matrix analysis is performed for the asymmetric chicane-type EEX beam line and an emittance dilution formula is derived analytically. The simulations were performed to benchmark against the theoretical prediction. The coherent synchrotron radiation (CSR) effect to the emittance dilution is also checked out.

* Corresponding author.
E-mail address: jiangbocheng@sinap.ac.cn (B.-C. Jiang).

http://dx.doi.org/10.1016/j.nima.2014.06.079

2. Transfer matrix of asymmetric EEX beam line

2.1. Beam transfer matrix

The asymmetry chicane-type EEX beam line is similar to telescope EEX beam line [12] as shown in Fig. 1. Two focusing quadrupoles Q1, Q2 with focal lengths $f1$ and $f2$ are placed in front of the deflecting cavity. The space between them is $f1+f2$. And a pair of focus–defocus quadrupoles Q3, Q4 with focal lengths $f3$ and $-f4$ are placed behind the cavity. The space between them is $f3-f4$. We define

$$N_1=\frac{f_2}{f_1}. \tag{1}$$

$$N_2=\frac{f_3}{f_4} \tag{2}$$

If $f_3=f_4$, N_2 will equal to 1 and Q3, Q4 will be vanished.

Two bending magnets with opposite magnet field with a drift space in between (half of the chicane) is called a dogleg [1]. The transfer matrix (only horizontal and longitudinal planes are considered) of the dogleg is shown in Eq. (3) and the transfer matrix of deflecting cavity for thin lens approximation can be written in Eq. (4).

$$R_{L1,2}=\begin{bmatrix}1 & L_{1,2} & 0 & \eta_{1,2}\\ 0 & 1 & 0 & 0\\ 0 & \eta_{1,2} & 1 & \xi_{1,2}\\ 0 & 0 & 0 & 1\end{bmatrix}, \tag{3}$$

$$R_{Cthin}=\begin{bmatrix}1 & 0 & 0 & 0\\ 0 & 1 & k & 0\\ 0 & 0 & 1 & 0\\ k & 0 & 0 & 1\end{bmatrix}, \tag{4}$$

where subscript 1, 2 denotes the first and the second dogleg, respectively. $L_{1,2}=(2L_{b1,2}cos\theta_{1,2}+D_{1,2})/\cos^2(\theta_{1,2})$ [13], $L_{b1,2}$ are the bending magnets' lengths, $\theta_{1,2}$ is the bending angle, $D_{1,2}$ is the drift space between the bending magnets, $\eta_{1,2}$ and $\xi_{1,2}$ are the dispersion and momentum compaction function of doglegs.

The transfer matrix of quadrupole doublets prior to and after the deflecting cavity can be respectively written under here,

$$R_B=\begin{bmatrix}-N_1 & a & 0 & 0\\ 0 & -1/N_1 & 0 & 0\\ 0 & 0 & 1 & 0\\ 0 & 0 & 0 & 1\end{bmatrix}, \tag{5}$$

$$R_D=\begin{bmatrix}1/N_2 & b & 0 & 0\\ 0 & N_2 & 0 & 0\\ 0 & 0 & 1 & 0\\ 0 & 0 & 0 & 1\end{bmatrix}, \tag{6}$$

where

$$a=f_1+f_2-N_1L_1-L_2/N_1, \tag{7}$$

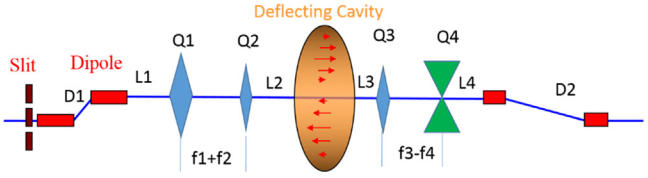

Fig. 1. The slit is imposed at the entrance of the EEX beam line.

$$b=f_3-f_4+N_2L_4+L_3/N_2. \tag{8}$$

To match an exact EEX, we needs:

$$\eta_1 k=\frac{1}{N_1}, \tag{9-1}$$

$$\eta_2 k=-1/N_2. \tag{9-2}$$

Multipling matrixes of the different sectors and substituting Eqs. (9-1, 9-2), the transfer matrix of the whole beam line can be written as

$$R=\begin{bmatrix}0 & 0 & k(b+L_2N_2) & -\frac{1}{kN_2}+k(b+L_2N_2)\xi_1\\ 0 & 0 & kN_2 & kN_2\xi_1\\ -kN_1\xi_2 & \frac{1}{kN_1}+k(a-L_1N_1)\xi_2 & 0 & 0\\ -kN_1 & k(a-L_1N_1) & 0 & 0\end{bmatrix}. \tag{10}$$

The 4×4 matrix R in Eq. (10) is constructed from four 2×2 blocks [2], A, B, C, and D as follows

$$R=\begin{bmatrix}A & B\\ C & D\end{bmatrix}, \tag{11}$$

where

$$A=\begin{pmatrix}R_{11} & R_{12}\\ R_{21} & R_{22}\end{pmatrix}, B=\begin{pmatrix}R_{13} & R_{13}\\ R_{23} & R_{24}\end{pmatrix}, \text{etc.}$$

The emittance exchange can be therefore written as [2],

$$\varepsilon_x^2=|A|^2\varepsilon_{x0}^2+|B|^2\varepsilon_{z0}^2+tr\{(A\sigma_xA^T)^aB\sigma_zB^T\}, \tag{12}$$

$$\varepsilon_z^2=|C|^2\varepsilon_{x0}^2+|D|^2\varepsilon_{z0}^2+tr\{(C\sigma_xC^T)^aD\sigma_zD^T\}, \tag{13}$$

where ε_x, ε_z are the transverse and longitudinal emittances respectively, A^a is the adjoint (or symplectic conjugate) of A. $|A|$ is determinant of A and $tr\{\}$ is the trace of the matrix.

With $\sigma_x=\begin{bmatrix}\varepsilon_{x0}\beta_{x0} & -\varepsilon_{x0}\alpha_{x0}\\ -\varepsilon_{x0}\alpha_{x0} & \varepsilon_{x0}\gamma_{x0}\end{bmatrix}, \sigma_z=\begin{bmatrix}\varepsilon_{z0}\beta_{z0} & -\varepsilon_{z0}\alpha_{z0}\\ -\varepsilon_{z0}\alpha_{z0} & \varepsilon_{z0}\gamma_{z0}\end{bmatrix}.$

It can be found out that (where subscript 0 means input bunch parameters):

$$|A|^2=|D|^2=0, \tag{14}$$

$$|B|^2=|C|^2=1, \tag{15}$$

$$tr\{(A\sigma_xA^T)^aB\sigma_zB^T\}=tr\{(C\sigma_xC^T)^aD\sigma_zD^T\}=0. \tag{16}$$

Eqs. (14)–(16) means that an exact emittance exchange between transverse and longitudinal planes has been achieved.

For a thick lens approximation, the beam transfer matrix of the cavity can be written into [2]:

$$R_C=\begin{bmatrix}1 & Lc & kLc/2 & 0\\ 0 & 1 & k & 0\\ 0 & 0 & 1 & 0\\ k & kLc/2 & k^2Lc/4 & 1\end{bmatrix}, \tag{17}$$

where Lc is the length of the cavity. The transfer matrix for the whole beam line is given by

$$R=\begin{bmatrix}0 & \frac{-Lc}{4N_1N_2} & \frac{kLc}{4N_2}+k(b+L_2N_2) & \frac{-4+k^2(Lc+4N_2b+4N_2^2L_2)\xi_1}{4kN_2}\\ 0 & 0 & kN_2 & kN_2\xi_1\\ -kN_1\xi_2 & \frac{4-k^2(Lc+4N_1^2L_1-4N_1a)\xi_2}{4kN_1} & \frac{k^2Lc\xi_2}{4} & \frac{k^2Lc\xi_1\xi_2}{4}\\ -kN_1 & -\frac{k(Lc+4N_1^2L_1-4N_1a)}{4N_1} & \frac{k^2Lc}{4} & \frac{k^2Lc\xi_1}{4}\end{bmatrix}. \tag{18}$$

The matrix also fulfils Eqs. (15) and (16). However the emittance dilution terms, i.e. the third terms in right hand side of Eqs. (12) and (13) do not vanish.

From the transfer matrix Eq. (18) we will find an x and σ phase space exchange can be reached by setting:

$$Lc+4N_1^2L_1-4N_1a=0. \tag{19}$$

2.2. Emittance dilution effects

The third term in right hand side of Eq. (12) and Eq. (13) are the emittance dilution terms. Respecting to matrix Eq. (18), the emittance dilution can be expressed as follows,

$$tr\left\{(A\sigma_xA^T)^aB\sigma_zB^T\right\}=\frac{k^2L_c^2\gamma_x\varepsilon_{x0}\varepsilon_{z0}[\beta_{z0}+(-2\alpha_{z0}+\gamma_{z0}\xi_1)\xi_1]}{16N_1^2}. \tag{20}$$

$$tr\left\{(C\sigma_xC^T)^aD\sigma_zD^T\right\}=\frac{k^2L_c^2\varepsilon_{x0}\varepsilon_{z0}[\beta_{z0}+(-2\alpha_{z0}+\gamma_{z0}\xi_1)\xi_1][\gamma_{x0}+4k^2N_1^2\xi_2(\alpha_{x0}+4k^2N_1^2\beta_{x0}\xi_2)]}{16N_1^2}. \tag{21}$$

From Eq. (20) and Eq. (21), we can find that

$$\beta_{z0}+(-2\alpha_{z0}+\gamma_{z0}\xi_1)\xi_1\approx 0, \tag{22}$$

can be reached to reduce the emittance dilutions both for transverse and longitudinal planes. To match this, the inject beam energy chirp should be optimized to match with ξ_1. The longitudinal emittance dilution is more complex with an additional term $\gamma_{x0}+4k^2N_1^2\xi_2(\alpha_{x0}+4k^2N_1^2\beta_{x0}\xi_2)$ which is a hyperbolic curve function of β_{x0} and parabola curve function of α_{x0}. Thus the longitudinal emittance dilution will be sensitive both to the transverse and longitudinal Twiss parameters of the inject bunch. It is interesting that emittance dilution terms only sensitive to N_1 and gets no N_2 contributions.

3. Simulation of the emittance exchange

3.1. Emittance dilutions versus to Twiss parameters

The tracking code Elegant [14] has been chosen for our simulations. An asymmetric chicane-type EEX beam line is setup with parameters listed in Table 1.

The doublets prior to the deflecting cavity were optimized to match Eq. (19) to make sure a phase space manipulation can be performed.

As a practical example we carried out a study by using the initial bunch parameters from the Fermi@Elettra injector [15]. The main parameters are listed in Table 2. 1×10^5 macro-particles are generated randomly within the parameters listed in Table 2 for tracking.

A β_{z0}, α_{z0} scan for emittance dilution is performed. As shown in Fig. 2 the minimum emittance dilution sits exactly at where Eq. (22) is matched.

Table 1
Main parameters of the EEX beam line.

	Preceding the cavity	Following the cavity
Quadrupole setting	$N_1=2$	$N_2=2.34$
Doglegs bending angle (θ)	0.2079 rad	0.1040 rad
Bending magnets length (L_b)	0.2 m	0.2 m
Drift between bends (D)	0.6 m	1.2 m
Dogleg η/ξ	0.1717 m/−0.0326 m	−0.1468 m/−0.0145 m
Deflecting cavity k	2.910 (~17.6 MV @95 MeV)	
Cavity length (L_c)	0.2 m	

Table 2
Main parameters of the inject bunch.

Bunch energy	95 MeV
Normalized emittance (x/z)	1.5/3.7 mm mrad
Energy spread (uncorrelated/correlated)	2 keV/~150 keV
Bunch length	700 fs

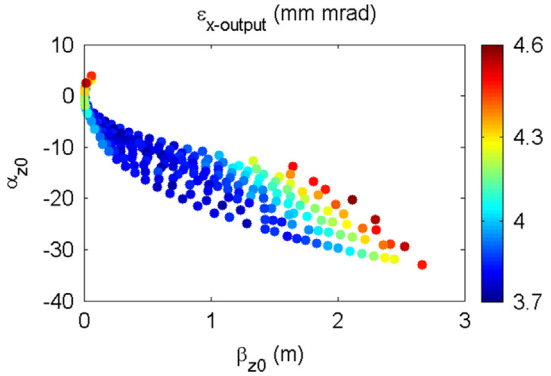

Fig. 2. Transverse emittance dilution caused by longitudinal Twiss parameters (Minimum emittance dilution sits at $\beta_{z0}+(-2\alpha_{z0}+\gamma_{z0}\xi_1)\xi_1\approx 0$, where $\xi_1=-0.0326$).

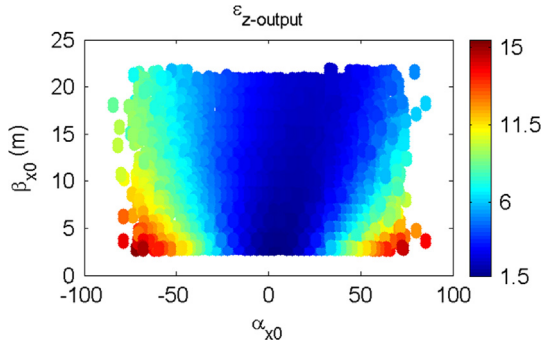

Fig. 3. Longitudinal emittance dilution caused by transverse Twiss parameters.

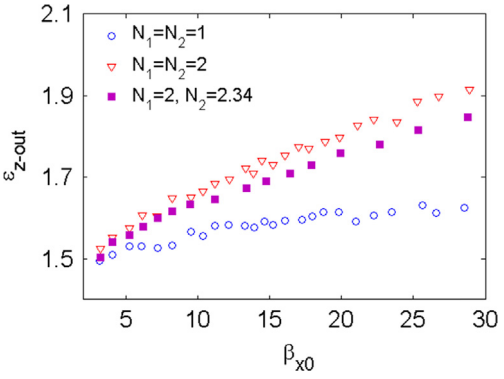

Fig. 4. Minimal longitudinal emittance achieved at different β_{x0}.

In the tracking, for the finite step sizes of β_{z0}, α_{z0} and the random creation of macro-particles, even for an optimized β_{z0}, α_{z0}, left hand side of Eq. (22) could not exactly equal to zero, longitudinal emittance dilution caused by β_{x0}, α_{x0} will also be found as shown in Fig. 3.

For energy bands creation, a multi-slit mask is placed at the entrance. A bigger beam size is favorable for relaxing the manufacture challenges. As to investigate emittance dilutions caused by β_{x0}, a chicane-type EEX with $N_1=N_2=1$ ($\xi_1=\xi_2=-0.1189$ m) and a telescope EEX beam line with $N_1=N_2=2$ ($\xi_1=\xi_2=-0.0326$ m) is

also simulated for comparison. The longitudinal emittance dilution can be affected both by N_1 and ξ_2 as predicted by Eq. (21). Fig. 4 shows for a fixed β_{x0}, the minimum longitudinal emittance dilution that can be achieved by scanning other parameters α_{x0}, α_{z0}, β_{z0}, which well agrees with the prediction of Eq. (21).

3.2. Energy bands creation and CSR effects

A multi-slit mask is place at the entrance of the EEX beam line as shown in Fig. 1, which is used to segment the incident bunch into a series of beamlets separated in horizontal position. With

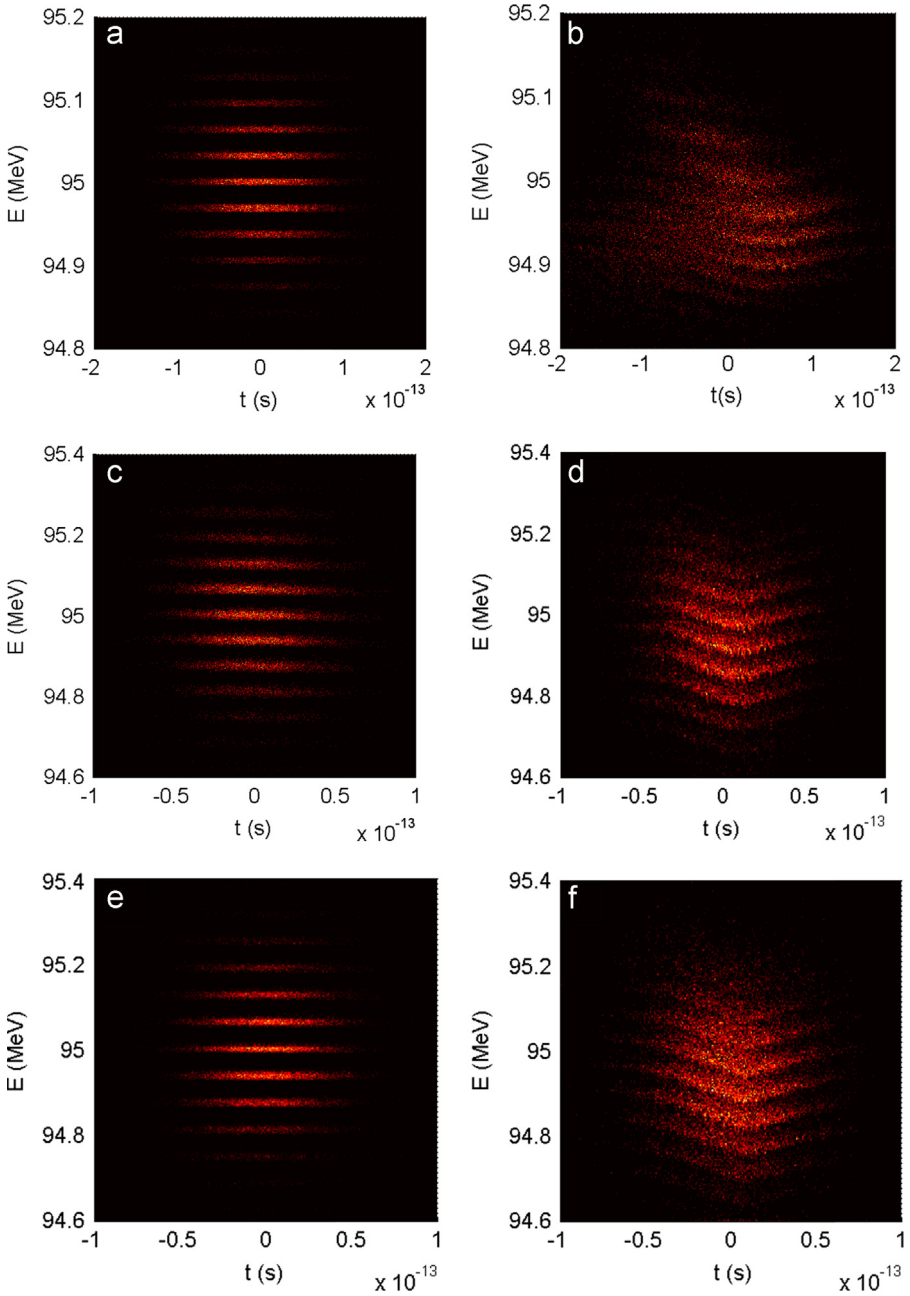

Fig. 5. Energy bands creation with a multi-slit mask at the entrance of the EEX beam line (a) $N_1=N_2=1$, no CSR effect; (b) $N_1=N_2=1$, 50 pC charge with CSR effect; (c) $N_1=N_2=2$, no CSR effect; (d) $N_1=N_2=2$, 50 pC charge with CSR effect; (e) $N_1=2$, $N_2=2.34$, no CSR effect; (f) $N_1=2$, $N_2=2.34$, 50 pC charge with CSR effect).

Table 3
Output beam parameters.

	$N_1=N_2=1$	$N_1=N_2=2$	$N_1=2$, $N_2=2.34$
Emittance x/z (without CSR) (mm mrad)	~3.7/1.5	~3.7/1.5	~3.7/1.5
Emittance x/z (with CSR) (mm mrad)	4.66/2.20	4.55/1.63	4.25/1.65
Bunch length (without CSR) (fs)	45	23	23
Energy spread of an energy band (without CSR) (keV)	2.3	6.6	5.1
Total energy spread (without CSR) (keV)	57.9	115.4	115.2

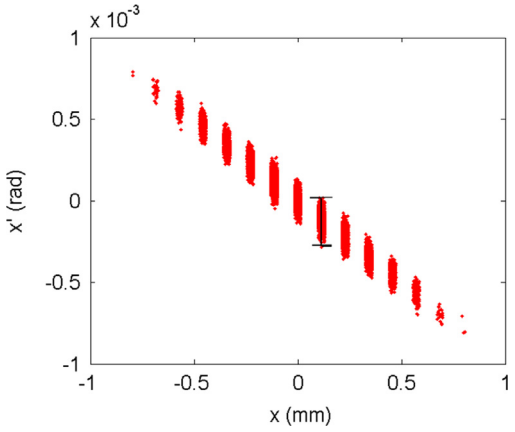

Fig. 6. Phase space of inject bunch.

phase space manipulation by the EEX beam line, the energy bands will be created in the output bunch. With further energy modulation by a laser in an undulator and chicane suppression, the temporal density modulation will be created which will contain higher harmonics of the seed laser. For this scheme, the energy bands retaining is of great importance. The energy bands can be smeared out by both the emittance dilution effects and CSR effect.

Three cases as that used for Fig. 3 are compared of energy bands creation. In the tracking without CSR effect the energy bands can be created distinctly as show in Fig. 5a, c and e, respectively. For all of these three cases, emittances are nearly exactly exchanged, namely $\varepsilon_{x\_out} \approx 3.7$ μm, $\varepsilon_{z\_out} \approx 1.5$ μm. The output bunch length (energy chirp) can be controlled by regulating α_{x0}. For Fig. 5a, at the optimized point, bunch length is reduced to 45 fs which is more than an order of magnitude lower than the inject bunch length 700 fs while for Fig. 5c and e, the bunch length is 24 fs and 23 fs, respectively. A summary of the output beam parameters is listed in Table 3.

4. Discussions and summary

In the EEX simulations, a remarkable bunch length suppression had been observed. The reason is that inject bunch is an ideal Gaussian bunch with linear x–x' correlation as shown in Fig. 6 which allows an ideal bunch length suppression. For a real bunch, the conditions may be more complicated and the output bunch length will be longer. Even though the feature of EEX is valuable because of tailoring transverse phase space of an injection bunch is much more convenient than that for a longitudinal phase space such as a chicane based bunch length suppression.

When approaching to bigger N_1 for further reducing the CSR effect and shortening the bunch length (which is preferred for FEL and plasma wakefield acceleration study), the emittance dilution will be more sensitive to β_{x0} as indicated in Fig. 4. EEX-HHG needs a multislit mask for energy bands creation, when considering the mechanical process, a bigger beam size (a bigger β_{x0}) is favorable. The final amplification factor N_1 will be a compromise of technical capability and beam dynamics acceptance.

So far the beam dynamics in the vertical plane are ignored. As shown in Fig. 1, three successive focus quadrupoles are arranged in the beam line, when looking into vertical plane, they are defocus quadrupoles, this requires a strong focus in vertical plane for the inject bunch (a big α_{y0}). Fig. 7 shows the beta function evolution along the EEX beam line for the asymmetric case for which $\alpha_{y0} = 46.7$ and the beta function of both ends are beyond 40 m and Fig. 8 shows output bunch transverse phase space. When approaching bigger N_1 and N_2, the focusing capability in vertical plane will be a concern.

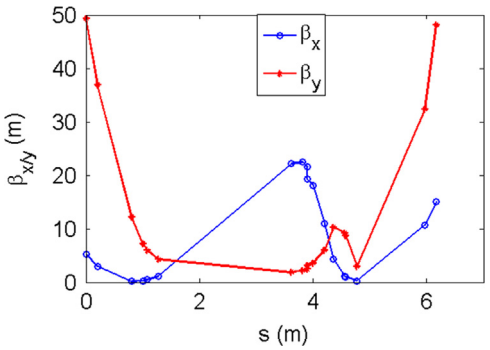

Fig. 7. β Function evolution along the beam line.

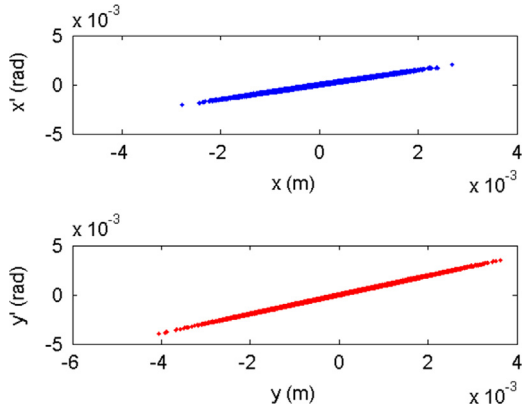

Fig. 8. Transverse phase space of output bunch.

Acknowledgments

The author would like to thank Dr. Guoxing Xia for useful helps. This work was supported by National Natural Science Foundation of China under Grant no. 11105214.

References

[1] P. Emma, et al., Phys. Rev. Spec. Top. Accel Beams 9 (2006) 100702.
[2] M. Cornacchia, P. Emma, Phys. Rev. Spec. Top. Accel. Beams 5 (2002) 084001.
[3] K.-J. Kim, A. Sessler, AIP Conf. Proc 821 (2006) 115.
[4] D. Xiang, Phys. Rev. Spec. Top. Accel. Beams 13 (2010) 010701.
[5] A. Johnson et al., in: Proceedings of IPAC'10, Kyoto, Japan, 4614–4616, 2010.
[6] Y.-E. Sun, et al., Phys. Rev. Lett. 105 (2010) 234801.
[7] B.E. Carlsten, et al., Phys. Rev. Spec. Top. Accel. Beams 14 (2011) 084403.
[8] B. Jiang, et al., Phys. Rev. Lett. 106 (2011) 114801.
[9] D. Xiang, AIP Conf. Proc. 1507 (2012) 120.
[10] B. Jiang, et al., Phys. Rev. Spec. Top. Accel. Beams 15 (2012) 011301.
[11] G. Stupakov, Phys. Rev. Lett. 102 (2009) 074801.
[12] D. Xiang, Alex Chao, Phys. Rev. Spec. Top. Accel. Beams 14 (2011) 114001.
[13] Y.-E. Sun et al., in: Proceedings of PAC07, New Mexico, USA, 3441–3443, 2007.
[14] M. Borland, elegant: A Flexible SDDS-Compliant Code for Accelerator Simulation, Advanced Photon Source LS-287, September 2000.
[15] C.J. Bocchetta et al., ELETTRA Report No. ST/F-TN-07/12, 2007.